21st Australasian Fluid Mechanics Conference
Adelaide, Australia
10-13 December 2018

Spatial Development of Trailing Vortices in the Far-Wake of a Delta Wing

S. E. Morris and C. H. K. Williamson

Sibley School of Mechanical and Aerospace Engineering
Cornell University, Ithaca, New York 14853, United States of America

Abstract

In this research we study the trailing vortices behind a 75° leading-edge sweep-angle delta wing, at 15° angle of attack. The delta wing is towed in an XY-Towing tank, generating a spatially developing vortex pair that has significant streamwise (axial) flow in the vortex cores. PIV using a transverse light sheet (perpendicular to the length of the vortices) is used to find the transverse velocity field, and to characterize the vortices using the superposition of two Lamb–Oseen vortices. The axial flow is captured using a longitudinal light sheet (parallel to the length of the vortices). In order to ensure we capture the vortex core, a novel technique is used wherein the light sheet is set such that it is slightly oblique to the length of the vortex. Using this technique allows the streamwise velocity profiles to be captured over 20 chord-lengths downstream of the delta wing. When the vortex pair is in ground effect, the boundary layer that forms on the surface between the vortices and the wall separates, generating secondary vorticity and causing the primary pair to 'rebound' in the same manner as is seen in temporally evolving vortex pairs [4]. Using this technique, our measurements are unaffected by vortex core movements. We can therefore analyse the axial flow profile both in and out of ground effect; to the authors' knowledge, the axial flow profile of the vortex pair in ground effect has not been previously measured experimentally. A Gaussian velocity profile with a wake-like velocity deficit (flow upstream) is observed in the far-wake of the delta wing in both cases. We also trigger the long-wavelength instability [1] in the vortices, and compare the measured growth rate of the instability to theory.

Introduction

Understanding vortex-wall interactions has applications in fundamental turbulence, as well as being of interest in the context of airplane trailing vortices. Counter-rotating aircraft wake vortices are an unavoidable by-product of lift, and can persist for long distances downstream of the aircraft. These vortices pose an increased hazard for following aircraft, as another aircraft flying through a vortex wake can experience dangerous rolling moments. This hazard is even more prevalent in air traffic take-offs and landings, as there is often insufficient altitude to recover.

Although seemingly simple, vortex pairs can produce complex three-dimensional dynamics due to instabilities and interactions with walls. Vortex pairs out of ground effect can become unstable to short-wave [11] or long-wave [1] instabilities. For the long-wave instability, the vortex cores experience a bending displacement mode. Each vortex tube initially bends in a sinusoidal fashion, growing in amplitude due to the mutual interaction of the two vortices. This amplitude increases until the vortices reconnect, transforming the vortex pair into a series of descending vortex rings [4].

Crow [1] determined the growth rate of the instability for a pair of Rankine vortices, as a function of the instability wavelength and the vortex core radius. Widnall *et al*. [11] extended this analysis to account for more general vortex profiles. By incorporating the concept of an *effective* core radius, a Rankine vortex with the same self-induced dynamics as the original vortex profile can be calculated, taking into account both the azimuthal and axial velocity profiles. This equivalent Rankine vortex core radius can be used in Crow's growth rate analysis to accurately predict the growth rate of the long-wave instability in vortex pairs with axial flow [4,5,6,8].

Wake-like axial flows have been observed in the cores of vortices in a number of experiments [e.g. 2,6,8]. However, vortex wandering can make it difficult to accurately obtain the axial velocity profile. Vortex wandering is the movement of the vortex core in random, side-to-side motions, relative to a fixed observer. These movements make it difficult to ensure that experimental measurements are intersecting the vortex core. As such, corrections must be made to account for the movement of the vortex core if techniques such as fixed hot-wire anemometry or PIV light sheets parallel to the vortex core are used [2].

This problem is augmented for a counter-rotating vortex pair in ground effect, as such a pair will rebound away from the ground upon wall interaction. This phenomenon was explained by Harvey and Perry [3] as a result of the generation of secondary vorticity at the wall. When a vortex pair approaches a ground plane, a boundary layer forms at the wall that is subject to an adverse pressure gradient. This boundary layer can then separate from the wall, rolling up to generate secondary vortices of opposite sign vorticity and causing the primary vortex pair to rebound. This rebound results in transverse displacements of the primary vortices; for a vortex pair with initial vortex spacing b_0, the final vortex spacing can be as much as $3b_0$.

In this work we use a technique to measure the axial flow that is unaffected by vortex core movements, and so can be applied to vortex pairs in ground effect. By towing a delta wing through a stationary light sheet and applying Taylor's hypothesis to convert from time to distance downstream ($x = tu_\infty$), we are able to obtain transverse and longitudinal data as close as 0.034 chord lengths apart; this resolution is significantly better than what has been achieved in previous studies, wherein axial flow measurements are commonly taken 3-5 chord-lengths apart (e.g. Devenport *et al.* and Roy *et al.* [2,8]). This allows us not only to find the shape of the axial flow profile, but also the variation in peak core velocity as a function of distance downstream, both in and out of ground effect. Using the axial flow data for a vortex pair out of ground effect, we also find the effective core radius to accurately predict the growth rate of the Crow instability.

Experimental Methods

Experiments were conducted using the Cornell University *Fluid Dynamics Research Laboratories* XY-Towing Tank. The towing tank is approximately 6m long, and has computer-controlled X and Y degrees of freedom. A delta wing with span s = 6cm is lowered into the tank and is held in position with thin wires; the wires that hold the delta wing in position have a diameter of 0.012" and do not generate a vortex wake. Similarly, the struts are streamlined to minimise any disturbances and are placed far enough from the delta wing to not affect the trailing vortices. The Reynolds number is defined by the chord length, c, of the delta wing and is defined in equation (1)

$$Re = \frac{u_\infty c}{\upsilon} \quad (1)$$

where u_∞ is the towing velocity. Experiments are run at *Re* = 5000 unless otherwise stated. As the delta wing is towed through the tank, a pair of counter-rotating vortices are generated. These vortices travel downward in the tank under their own self-induction. The facility also includes a transparent, horizontal acrylic ground plane that can be submerged in the tank for experiments in ground effect.

A powerful feature of this facility is the ability to trigger the Crow [1] instability, by introducing small perturbations in the towing velocity. This is achieved by implementing a sinusoidal fluctuation to the towing velocity as given by equation (2)

$$u(t) = u_\infty + u' \sin\left(2\pi \frac{u_\infty t}{\lambda_f}\right) \quad (2)$$

where u'/u_∞ is the normalised forcing amplitude (1–10%) and λ_f/b_0 is the instability wavelength [6].

Two different techniques are used to analyse the flow: laser induced fluorescence dye visualization, and PIV. For flow visualization, fluorescein dye is illuminated by a Coherent Innova 90 argon-ion laser. The flow can either be floodlit for a view of the entire flow, or a cross-section can be illuminated. Dye is applied directly to the delta wing to observe the trailing vortices. Images are acquired with an intervalometer-controlled digital single lens reflex (DSLR) camera at a rate of 1 Hz.

PIV is used to obtain quantitative measurements of the flow, in both the transverse and longitudinal planes. A charge-coupled device (CCD) Jai CV-M2CL camera is used to capture image pairs at a rate of 13Hz. Velocity fields are calculated by processing the image pairs using PIVLab software [10].

Using the transverse plane, the vertical (azimuthal) velocity of the vortex pair is well-modelled by the superposition of two Lamb–Oseen vortices. By applying a least-squares best fit of this superposition to our transverse velocity data, we can determine the circulation, Γ, the vortex core size, a, and b_0. The azimuthal velocity profile of each Lamb–Oseen vortex is given by equation (3)

$$v_\theta(r) = \frac{\Gamma}{2\pi r}\left[1 - exp\left(-\frac{r^2}{a^2}\right)\right] \quad (3)$$

where r is the distance measured from the vortex centre. The vortex core size is defined as $a = 1.12r_1$, where r_1 is the location at which the circumferential velocity v_θ is a maximum; r_1 grows according to viscous diffusion [9], given by equation (4)

$$r_1(t) = 2.24\sqrt{\nu(t + t_0)} \quad (4)$$

where t_0 is the virtual origin. For our delta wings with s = 6cm, the ratio of initial core size to vortex spacing is a_0/b_0 = 0.25.

Flow Visualization of Trailing Vortices

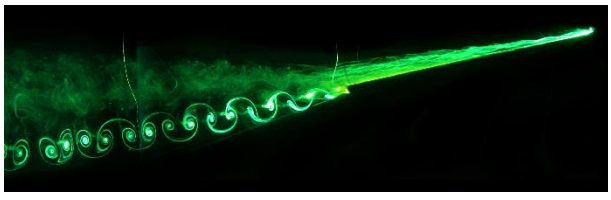

Figure 1. Cross-sectional view of the braid wake behind a delta wing at Re = 10 000.

We visualize the trailing vortices using laser induced fluorescence dye visualization. In addition to a counter-rotating vortex pair behind the delta wing, Miller and Williamson [7] observed the presence of a "braid wake" behind the trailing edge, with its form dependent on Reynolds number. Figure 1 shows a cross-sectional view down the centre longitudinal plane of the delta wing, highlighting this braid wake. At *Re* = 10 000, a distinct von Kàrmàn vortex street is observed.

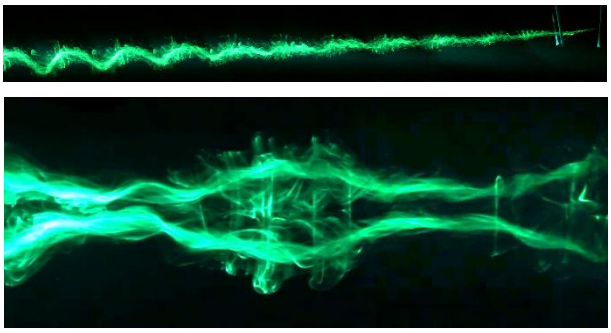

Figure 2. Side view (upper) and plan view (lower) of trailing vortices subject to the Crow instability. Side view shows the development of the waviness of the Crow instability downstream of the delta wing. Plan view shows a close up of a vortex ring.

In addition to studying unperturbed vortex pairs, we also examine a vortex pair subject to the long-wavelength instability. Figure 2 shows the instability developing downstream of the delta wing. The amplitude of the instability grows, until the point at which the primary vortices reconnect and form a series of vortex rings. By obtaining the axial flow velocity of the primary vortices via PIV, an accurate comparison of the growth rate to theory can be made.

PIV of Vortex Pairs In and Out of Ground Effect

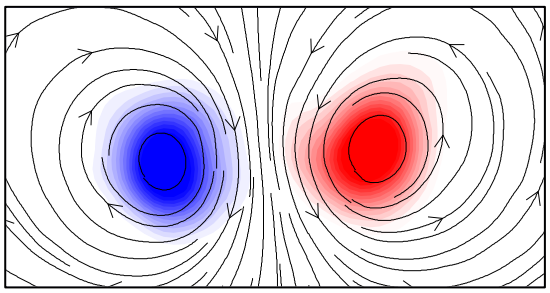

Figure 3. Vorticity contours and streamlines of a trailing vortex pair out of ground effect.

PIV is used to acquire quantitative flow measurements, with light sheets aligned in the transverse direction used to obtain a cross-section of the vortex pair. Figure 3 shows vorticity contours and streamlines of a vortex pair out of ground effect. When there is no wall present, the vortex pair will travel downward under its own self-induction.

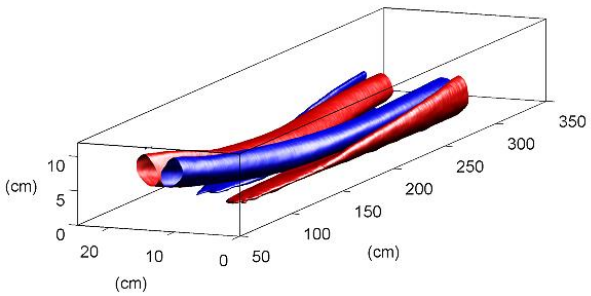

Figure 4. Vorticity isocontours of a vortex pair in ground effect.

For a vortex pair approaching a wall, the boundary layer that forms between the primary vortex and the wall separates, generating secondary vorticity and causing the primary vortices to 'rebound' [3]. Figure 4 shows vorticity isocontours of the

vortex pair in ground effect. We see the rolling up of secondary vorticity around the primary vortices, and the rebound of the primary vortex pair. We also observe the increase in vortex separation, b_0, between the two primary vortices as they move apart following ground interaction.

Axial Flow Measurement Technique and Results

A problem that arises in measuring axial flow in vortices is the need to correct for vortex wandering. For a vortex pair in ground effect, this problem is exacerbated. As each vortex pair can move up to an entire vortex spacing, fixed measurement techniques cannot be used. We therefore introduce a technique to measure axial velocity via PIV, that is unaffected by vortex core movements.

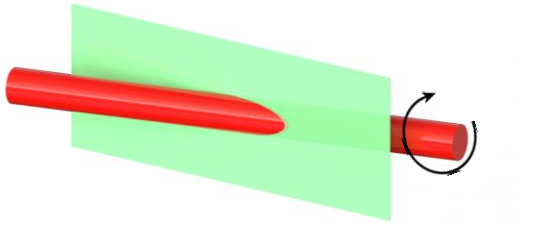

Figure 5. Schematic of the oblique-section technique [7]. The laser sheet is set at an angle offset to the tangent of the vortex core, such that the core is captured even when the vortex moves.

The concept of using an oblique light sheet was explored by Miller and Williamson in 1996 [7]. In this technique, the longitudinal laser sheet is set at an angle offset to the vortex core, as shown in figure 5. This ensures that the light sheet will intersect the core in the present work, even when the vortex core experiences transverse displacements.

Following PIV processing, axial flow in the vortex core is easily distinguishable in the resultant velocity field. This is due to the fact that the vortex core is the only location consisting solely of streamwise velocity vectors (no circumferential velocity component). At all other locations, the velocity vector has both streamwise and circumferential components due to the rotation of the vortex. The vectors with no circumferential velocity component therefore represent the vortex core.

The angle of the light sheet ensures that the vortex core is still captured, even when the vortex core moves in ground effect. When the vortex core experiences displacements, the location of streamwise velocity vectors will still remain within the large field of view. Accurate axial velocity profiles for vortices both in and out of ground effect can therefore be obtained more than 20 chord-lengths downstream. For our delta wing with s = 6cm, this equates to data over 2.2m downstream of the trailing edge!

Results for a Vortex Pair out of Ground Effect

Figure 6 shows the raw axial velocity measurements taken for a vortex pair out of ground effect. As the height of the measurement is shown on the y axis, we can see the vortex physically moving downward. The maximum axial velocity in the vortex core is well approximated by $u_0 \propto \frac{1}{\sqrt{t}}$, where u_0 is the maximum measured core velocity. A wake-like velocity deficit is seen in the vortex core: flow is moving upstream, towards the trailing edge of the delta wing. The axial flow is 44% the towing velocity at 2.9 chord-lengths downstream.

To confirm the validity of this technique, axial flow data at a number of downstream locations were fitted to the q-vortex solution for axial velocity [5]; this is a Gaussian profile given by equation (5)

$$v_z(r,t) = u_0(t)\left[exp\left(\frac{r^2}{a(t)^2}\right)\right] \qquad (5)$$

As shown in figure 7, the match between our data and equation (5) is excellent.

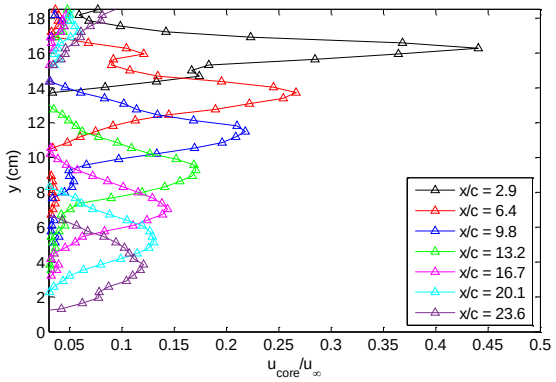

Figure 6. Axial velocity measurements up to 24 chord-lengths downstream, for a vortex pair out of ground effect. Data is shown at intervals of x/c = 3.4 for clarity.

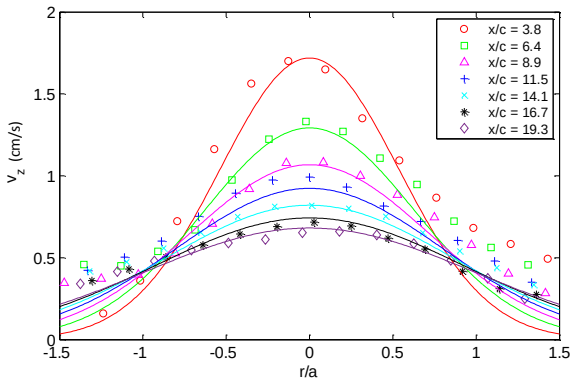

Figure 7. Axial velocity profiles, v_z, out of ground effect.

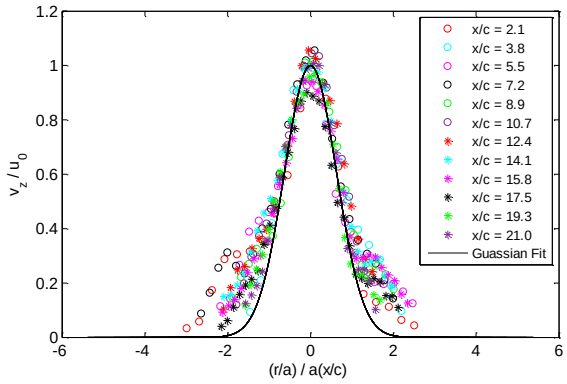

Figure 8. Axial velocity profiles normalised by the maximum axial velocity, and the vortex core size.

When the Gaussian velocity profiles are normalised by u_0 and a, the axial flow profile is self-similar, as shown by figure 8.

These axial velocity profiles can be used to determine the effective core radius as defined by Widnall *et al.* [11] to use in Crow's growth rate analysis for the long-wave instability. The effective core radius is defined in equation (6)

$$a_e = aexp\left(\frac{1}{4} - A + C\right) \qquad (6)$$

where A is a constant defined by the azimuthal (transverse) velocity profile, and C is defined by the axial (longitudinal) flow profile. Further details can be found in Leweke *et al.* [4].

For a vortex pair with a Lamb–Oseen transverse velocity profile and Gaussian axial flow, the effective core radius given by [4] is equivalent to equation (7)

$$a_e \approx 1.36aexp\left(\frac{1}{2}\left[\frac{u_0 2\pi a}{\Gamma}\right]^2\right) \quad (7)$$

For our vortex pair at *Re* = 5000, using the maximum axial velocity at the location at which the longwave instability is first apparent, $a_e \approx 0.45b_0$. This effective core radius, taking into account the measured axial flow, is significantly larger than the initial core radius, $a_o \approx 0.25b_0$. The growth rate, σ, of a vortex pair with 5% forcing amplitude is shown in figure 9.

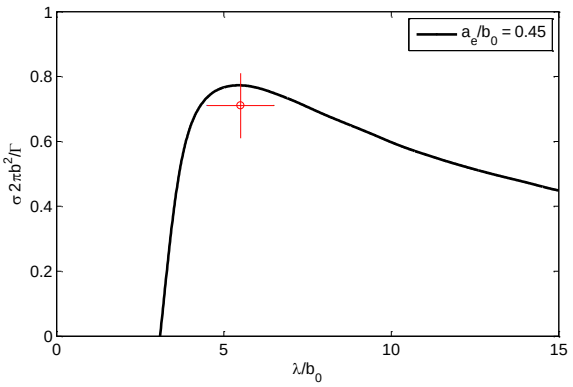

Figure 9. Comparison of the measured growth rate from flow visualization for a vortex pair with 5% forcing amplitude to the growth rate curve defined by Crow for $a_e = 0.45b_0$ [5,6].

Results for a Vortex Pair in Ground Effect

For a vortex pair in ground effect, we again observe a wake deficit in the vortex core. Whilst the velocity profile remains Gaussian, the vortex core size can no longer be described by equation (4). As such, we cannot use equation (5) to describe the velocity profile; rather, the axial flow profile for the vortex pair in ground effect must be defined using the full-width half-maximum (*FWHM*) determined from raw experimental data. This is given in equation (8)

$$v_z(r,t) = u_0(t)\left[exp\left(\frac{-4\ln 2r^2}{FWHM^2}\right)\right] \quad (8)$$

where $FWHM = 2\sqrt{2\ln(2)}\sigma$, and σ is the standard deviation. Preliminary results show that the *FWHM* of the vortex pair in ground effect remains up to 20% higher following ground interaction in comparison to an isolated vortex pair.

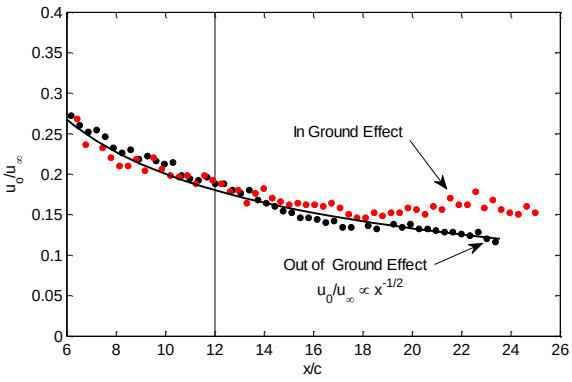

Figure 10. Maximum core velocity for a vortex pair out of and in ground effect. The solid line at *x*/c = 12 marks the locatio at which vortex-wall interactions begin.

A similar result is obtained when comparing the maximum axial velocity in the vortex core. Following ground interaction, the maximum axial velocity remains up to 20–30% higher for the vortex pair in ground effect for the recorded *x*/*c* values. Figure 10 shows the deviation of u_0 following wall interaction from the $u_0 \propto \frac{1}{\sqrt{x}}$ trend observed for a vortex pair out of ground effect.

Conclusions

The velocity profiles of vortex pairs both in and out of ground effect have been characterised. Using transverse PIV measurements, a least-squares best fit of our experimental data is applied to the superposition of two Lamb–Oseen vortices. A technique to obtain longitudinal velocity data that is unaffected by vortex core movements is used to measure the axial velocity, at a resolution of 0.034 chord-lengths. The isolated vortex pair is self-similar when normalised by the maximum core velocity and vortex core size, and self-similarity is observed as far as over 20 chord-lengths downstream; this equates to over 2.2m downstream of our 6cm span delta wing! For the vortex pair in ground effect, we find that we cannot use the same Gaussian velocity profile as is used for an isolated vortex pair; the full-width half-maximum and maximum axial velocity curves both remain up to 20% higher following wall interaction than what is observed for the vortex pair out of ground effect.

Using the axial velocity measurements of the isolated vortex pair at the time at which the long-wave instability is first initialised, we also find the effective core radius a_e to use in Crow's growth rate analysis. With this effective core radius, we see good agreement between the growth rate obtained by experiments and that predicted by theory.

References

[1] Crow, S. C., Stability Theory for a Pair of Trailing Vortices, *AIAA J.*, **39** (12), 1970, 2374–2381.

[2] Devenport, W. J., Rife, M. C., Liapis, S.I. & Follin, G. J., The structure and development of a wing-tip vortex. *J. Fluid Mech.*, **312**, 1996, 67–106.

[3] Harvey, J. K. & Perry, F. J., Flowfield produced by trailing vortices in the vicinity of the ground. *AIAA*. **9** (8), 1971, 1659–1660.

[4] Leweke, T., LeDizès, S. & Williamson, C. H. K., Dynamics and instabilities of vortex pairs. *Ann. Rev. Fluid Mech.* **48**, 2016, 1–35.

[5] Leweke, T. & Williamson, C. H. K., Experiments on long-wavelength instability and reconnection of a vortex pair. *Phys. Fluids*, **23**, 2011, 024101.

[6] Williamson, C. H. K., Leweke, T & Miller, G. D., Fundamental Instabilities in Spatially-Developing Wing Wakes and Temporally-Developing Vortex Pairs, in *Turbulence Structure and Vortex Dynamics*, editors: J. C. R. Hunt and J. C. Vassilicos, Cambridge University Press, 2000, 83–103

[7] Miller, G. D. & Williamson, C. H. K., Turbulence in the wake of a delta wing. *Proc. of Sixth European Turbulence Conference*, 1996.

[8] Roy, C., Leweke, T., Thompson, M. C. & Hourigan, K., Experiments on the elliptic instability in vortex pairs with axial core flow. *J. Fluid Mech.*, **677**, 2011, 383–416.

[9] Saffman, P. G., *Vortex Dynamics*, Cambridge University Press, 1993.

[10] Thielicke, W. & Stamhuis, E. J., Pivlab – time-resolved digital particle image velocimetry tool for matlab. Version: 1.40. 2014

[11] Widnall, S. E., Bliss, D. B. & Tsai, C.-Y., The instability of short waves on a vortex ring. *J. Fluid Mech.*, **66**, 1974, 35–47.